

Supersensitive Polarization Microscopy Using NOON States of Light

Yonatan Israel, Shamir Rosen, and Yaron Silberberg

Department of Physics of Complex Systems, Weizmann Institute of Science, Rehovot 76100, Israel

(Received 5 October 2013; published 12 March 2014)

A quantum polarized light microscope using entangled NOON states with $N = 2$ and $N = 3$ is shown to provide phase supersensitivity beyond the standard quantum limit. We constructed such a microscope and imaged birefringent objects at a very low light level of 50 photons per pixel, where shot noise seriously hampers classical imaging. The NOON light source is formed by combining a coherent state with parametric down-converted light. We were able to show improved phase images with sensitivity close to the Heisenberg limit.

DOI: 10.1103/PhysRevLett.112.103604

PACS numbers: 42.50.Dv, 06.30.Bp, 42.50.St

When imaging under low light conditions, one becomes particularly concerned with the effect of noise on the image. Since image sensitivity is classically limited by the shot noise, the natural approach is to increase image quality by simply raising the illumination power. With certain specimens, however, increasing the flux of the illuminating source is undesirable. Such is the case with photosensitive biological samples [1], quantum gases [2], and atomic ensembles [3]. In such circumstances one might consider resorting to nonclassical illumination where the contribution of each photon to the image contrast is enhanced. In this work we show that imaging sensitivity that surpasses that of any classical illumination source can be obtained by use of path-entangled states of N photons, commonly known as NOON states [4–6].

A photonic NOON state is a two-mode state in which N photons are in a superposition where all photons are in either one mode or the other. In Fock notation, this state is represented by

$$|\text{NOON}\rangle = \frac{1}{\sqrt{2}}(|N, 0\rangle_{D,A} + |0, N\rangle_{D,A}), \quad (1)$$

where D, A are two modes, which can be, for example, two orthogonal polarizations. These states are maximally entangled, and as such, they can be used to measure phase with enhanced sensitivity. In fact, NOON states are known to reach the Heisenberg limit in phase sensing [5,7]. One might consider exploiting this phase supersensitivity to enhance image quality in microscopy. Since all phase imaging techniques, such as phase-contrast microscopy and differential interference contrast microscopy, fundamentally rely on interference for conversion of phase shifts into brightness, they can all benefit from the use of entangled light. Here we report a scheme for quantum polarized light microscopy (QPLM) that uses NOON states for illumination.

While entangled states of light are commonly used to surpass the shot-noise limit in quantum metrology [7], their

use for sub-shot-noise imaging is in its infancy. Related works have demonstrated the use of quantum correlations of photon pairs to achieve sub-shot-noise imaging of an absorbing sample [8], as well as the use of squeezed light to enhance particle tracking sensitivity [9]. Only very recently, Ono *et al.* [10] reported quantum differential interference contrast imaging with entangled photon pairs, clearly demonstrating phase supersensitivity. In our study we investigated QPLM with $N = 2$ and $N = 3$ NOON states, in the limit of very low light illumination, about 50 photons per image element. Under such conditions the shot noise is significant, and the benefit of entanglement is quite obvious.

Polarized light microscopy (PLM) enables observation of transparent specimens that are nonisotropic and therefore can be made visible through their birefringence. Light passing through a birefringent sample accumulates a spatially dependent phase difference $\phi(x, y)$ between two orthogonal components of polarization, where x and y are the coordinates of the object plane. In a standard PLM the input light is linearly polarized, and the induced phase difference $\phi(x, y)$ leads to a rotation of polarization which is sensed by an analyzer, translating those phase differences into intensity patterns. Like any interferometric system, PLM using classical light sources is limited by the standard quantum limit, $\Delta\phi(x, y) \geq 1/\sqrt{N}$, which particularly affects the image quality at low light levels.

In order to surpass this limitation, we have constructed a microscope in which the sample is illuminated by a collinear NOON state, entangled in the two linear polarization modes. Photonic NOON states have been generated since the Hong-Ou-Mandel experiment [11], where two photons impinging on the two input ports of a beam splitter exit as a two-photon NOON state in the output ports. Higher-order NOON states (that is, with $N > 2$) are significantly more difficult to generate. Here we use a method, proposed by Hofmann and Ono [12], whereby a nearly perfect superposition of NOON states, scalable to

any order, is obtained by mixing coherent light (CS) with spontaneous parametric down-converted light (SPDC). This method was later used to experimentally demonstrate NOON states up to $N = 5$ [6]. We utilize this method now to generate $N = 2$ and $N = 3$ NOON states, in a proof-of-concept QPLM setup, to demonstrate and investigate beyond-classical phase microscopy supersensitivity.

The experimental setup is illustrated in Fig. 1. Superposition of NOON states in the mutually orthogonal modes D and A polarized at $\pm 45^\circ$ to the horizontal is created as in Ref. [6]. The incoming fluxes of CS and SPDC are set to yield 350 measured photon pairs per second from each (note that the CS contains about 2.5×10^5 additional unpaired photons per second). The total transmission of the setup for single photons, including the efficiency of the detectors, is measured to be 6.5%. A transparent birefringent sample of crystalline quartz powder in index matching oil introduces slight phase shifts [$\phi(x, y) \ll \pi$] between the two polarizations of the scanning beam.

The birefringence phase shift is encoded onto each of the NOON states resulting in

$$|\Psi_N\rangle = (|N, 0\rangle_{D,A} + e^{iN[\phi(x,y)+\phi]}|0, N\rangle_{D,A})/\sqrt{2}, \quad (2)$$

where ϕ is a controlled phase shift offset. Photon-number detection is performed at the horizontal (H) and vertical (V) polarization components. The probability for detecting exactly m photons in H and $N - m$ photons in V is

$$P_{m,N-m}(\phi(x, y)) = |\langle \Psi_N | m, N - m \rangle_{H,V}|^2, \quad (3)$$

for $m = 0, \dots, N$. These probabilities are known to exhibit superoscillations [6], and hence can increase the phase sensitivity. The phase estimate ϕ_{est} can be retrieved by inverting the calculated dependence $P_{m,N-m}(\phi)$. $\phi_{\text{est}} = \phi(P_{m,N-m})$ is then used as a calibration to estimate the phase at every point x, y in the sample, using the measured normalized coincidence rates, $P_{m,N-m}(x, y)$. The uncertainty associated with these estimates is

$$\Delta\phi_{m,N-m} = \frac{\Delta P_{m,N-m}}{\left| \frac{\partial P_{m,N-m}}{\partial \phi} \right|}, \quad (4)$$

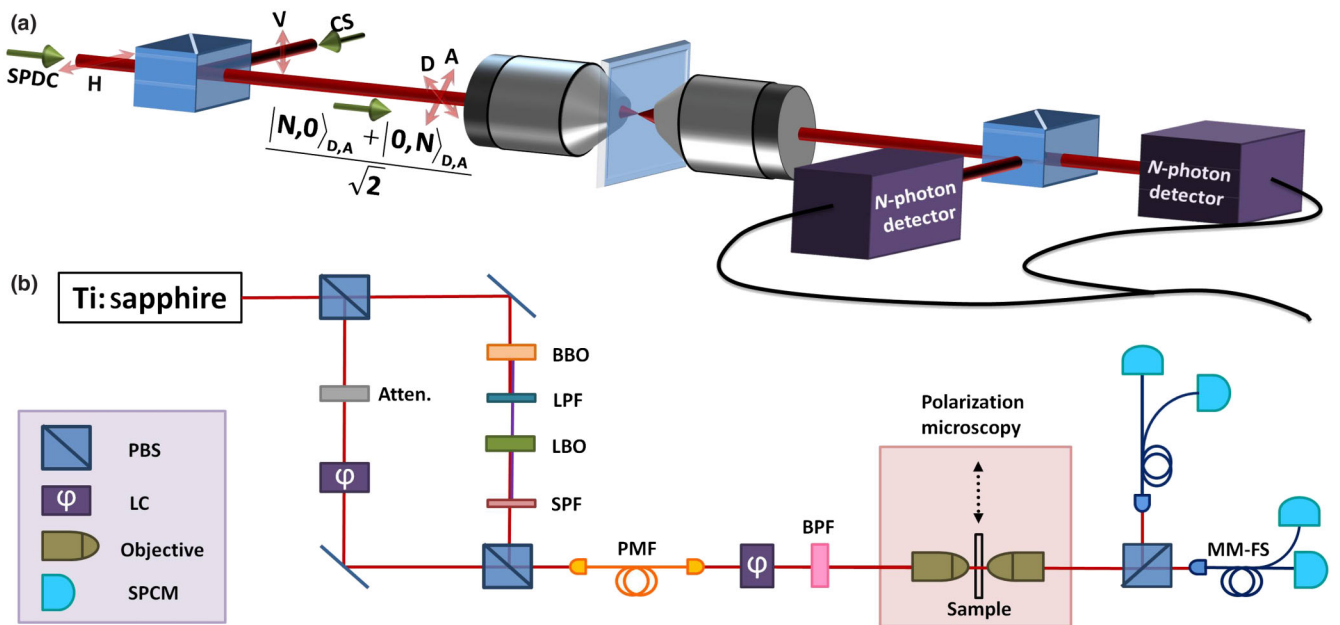


FIG. 1 (color online). Experimental setup. (a) Illustration of interferometric polarized light microscopy (PLM) using quantum states of light. The collinear Mach Zehnder (MZ) interferometer is fed by coherent light (CS) and spontaneous parametric down-converted light (SPDC) in its two input ports in polarizations H and V . The generated states, polarized at $\pm 45^\circ$ to the horizontal (D and A polarizations), are focused on a birefringent sample which is scanned by an X - Y stage. The states are then interfered at the second beam splitter of the MZ and measured in a photon-number-resolving apparatus. (b) Detailed layout of the setup. 120-fs pulses from a Ti:sapphire oscillator operated at 80 MHz are up-converted using a lithium triborate (LBO) crystal, short-pass filtered, and then down-converted using a beta barium borate (BBO) crystal, generating correlated photon pairs at the original wavelength (808 nm). This SPDC (H polarization) is mixed with attenuated coherent light (V polarization) on a polarizing beam splitter (PBS). A thermally induced drift in the relative phase is corrected every few minutes with the use of a liquid crystal (LC) phase retarder. The spatial and spectral modes are matched using a polarization-maintaining fiber (PMF) and a 3-nm (FWHM) bandpass filter (BPF). The MZ is polarization based in a collinear inherently phase-stable design. The PLM is realized with a pair of aspheric lenses (0.6 NA) which focus the light on a sample scanned by a piezostage (Physik Instrumente). The MZ offset phase is controlled using an additional LC phase retarder at 45° . Photon-number-resolving detection is performed using an array of single-photon counting modules (SPCM, Perkin Elmer).

where the uncertainty associated with $P_{m,N-m}$ is $\Delta P_{m,N-m} = (P_{m,N-m} - P_{m,N-m}^2)^{1/2}$ [5,13,14]. This uncertainty is bounded by the Heisenberg limit, $\Delta\phi_{m,N-m}(x, y) \geq 1/N$ [15], suggesting a potential \sqrt{N} enhancement over the sensitivity of classical phase microscopy. Repeated measurements with ν_N copies of the state reduce the total uncertainty to $\Delta\phi_{m,N-m}/\sqrt{\nu_N}$.

To take into account deviations from this ideal situation that are dictated by experimental limitations, we generated calibration curves for phase reconstruction using a numerically calculated theoretical model [6] for the coincidence rates as a function of φ , the phase difference between modes A and D . These calculations take into account the photon loss and detection inefficiencies in our setup, as well as the deviation of our source from a perfect NOON state source. Measured coincidence rates were obtained with no sample present, by varying φ using a liquid crystal retarder. Figures 2(a)–2(c) show measurements and calculations of coincidence rates in our setup for CS and for $N = 2$ and $N = 3$ states, which were then normalized to yield $P_{1,0}$, $P_{1,1}$, and $P_{2,1}$, respectively ($P_{3,0}$ and $P_{0,3}$ are nondetectable in our system, see Supplemental Material [15]). As expected, the NOON state correlations exhibit superoscillations. The phase uncertainty is then evaluated using Eq. (4), and the values for $\Delta\phi_{1,0}$, $\Delta\phi_{1,1}$, and $\Delta\phi_{2,1}$ are shown in Figs. 2(d)–2(f). These demonstrate that, even when the experimental imperfections are taken into account, the NOON states achieve phase supersensitivity, with minimum uncertainty values very close to the Heisenberg limit of $1/N$ [the shaded area in Figs. 2(d)–2(f)]. The actual minimum values are $\Delta\phi_{1,1}^{\min} = 0.559$ and $\Delta\phi_{2,1}^{\min} = 0.395$, and we attribute the deviation from the ideal $1/N$ values to the slightly impaired visibility of $N = 2$ and $N = 3$ NOON

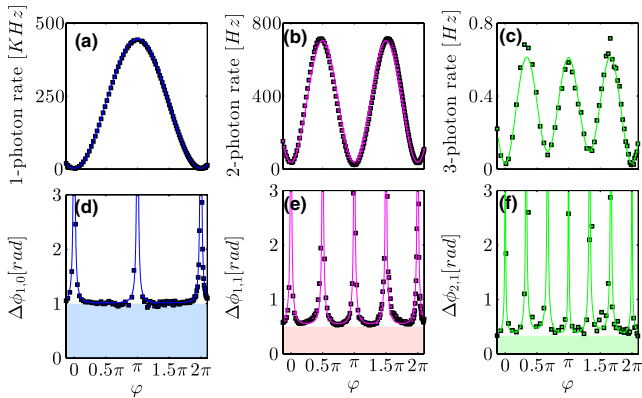


FIG. 2 (color online). Photon correlation and phase uncertainties. Measurements (squares) and theory (solid lines) of correlation rates in (a) CS, (b) $N = 2$, and (c) $N = 3$ NOON states are shown in blue, purple, and green, respectively. Measurement and theory of phase uncertainties (d) $\Delta\phi_{1,0}$, (e) $\Delta\phi_{1,1}$, and (f) $\Delta\phi_{2,1}$ are calculated for CS, $N = 2$, and $N = 3$ NOON states, respectively, by employing Eq. (4). Shaded areas are below the Heisenberg limit.

correlations, which is due to photon loss in higher NOON states [6].

Still, even these increased values are significantly better than $1/\sqrt{N}$ dictated by the standard quantum limit for classical light, leading to a reduction in the uncertainty by a factor of 0.79 and 0.68 for $N = 2$ and $N = 3$, respectively.

Figure 3 displays the phase images of a quartz crystal fragment reconstructed from correlation measurements made at every point in the sample. Figures 3(a)–3(c) show the phase image retrieved from measurements with CS and $N = 2$ and $N = 3$ NOON states using exactly 50 single photons, 25 pairs, and 17 triples, respectively, in each pixel. Figure 3(d) displays the same object obtained with bright CS illumination. In each of these images, the offset phase was set to be optimal in the sense that it confines the image phase range to that which can be sensed with minimal uncertainty. The relative offset phase was then subtracted from the images to make them more easily comparable. Juxtaposing Figs. 3(a)–3(c) indeed shows that NOON state illumination brings about considerable enhancement in the signal-to-noise ratio, which is clearly visible in line scans [Figs. 3(e)–3(h)], and also in the level of noise at the background regions. We note, on the other hand, that the $N = 3$ state is less accurate at the large phase values, because of the phase folding near $\pi/3$ dictated by the superoscillation.

In order to estimate the relative noise in the images, we chose an area in the image [marked by a black rectangle in

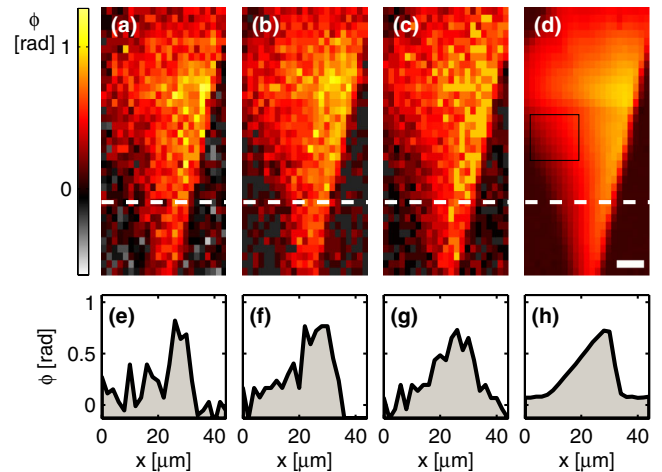


FIG. 3 (color online). Polarization microscopy images of a sample of single quartz crystal. (a)–(d) Comparison of phase microscopy sensitivity for quantum and classical illumination is presented by images using (a) CS only, (b) $N = 2$, and (c) $N = 3$ NOON states using exactly 50 single photons, 25 pairs, and 17 triples, respectively, in each pixel. (d) Reference image using bright illumination. The color bar represents phase in radians, and a white scale bar in (d) is $10 \mu\text{m}$. (e)–(h) Cross sections, marked by dashed white in (a)–(d), respectively. A black rectangle in (d) marks the area used for evaluating the noise in each of the images (a)–(d) (see text for more details).

Fig. 3(d)] at which the birefringence of the particle varies smoothly and is far from the singular points of the phase estimators, and therefore can be measured with the least uncertainty. We define local uncertainty (LU) as the root-mean-squared differences between each pair of neighboring pixels. This gives a measure of the noise in the image. The extracted values are $LU_{CS} = 0.208 \pm 0.136$, $LU_{N=2} = 0.177 \pm 0.110$, and $LU_{N=3} = 0.142 \pm 0.092$, where the $\pm\sigma$ values represent the statistical standard error. The reduction in noise and improvement in the image quality can be evaluated by $(LU_{N=2}/LU_{CS}) = 0.84 \pm 0.08$ and $(LU_{N=3}/LU_{CS}) = 0.68 \pm 0.07$. These values are in accordance with the expected enhancement values of 0.79 and 0.68, respectively, as discussed above.

Of course, when we state that the imaging was obtained with 50 photons per pixel, this was the number of photons detected in the relevant states that were used to extract image information. The number of photons passing through our sample was actually much higher, for two main reasons. First, our source does not provide pure NOON states. The use of a NOON state superposition and postselection, as we did here for demonstration purposes, is problematic since a significant fraction of the light is necessarily contained in lower-order states, and particularly in the lowest order of ($|1, 0\rangle + |0, 1\rangle$), thus illuminating the object with more photons than necessary. A similar problem would be encountered in schemes that use heralded NOON states. A single-order high-NOON state source would allow greater fractions of enhancements in phase imaging sensitivities, but in effect all high-NOON sources demonstrated to date are either heralded or in a superposition state [4,6,16].

However, even if pure high-NOON state sources were available, loss would be a serious issue. NOON states are notoriously sensitive to photon loss. An imaging system with total quantum efficiency of η for transmission and detection of a single photon will use only η^N of the N -photon NOON states, again leading to many useless photons passing through the sample. Hence, transmission of the setup should be maximized, and incorporation of more efficient photon-number-resolving detectors is crucial; we note that detection efficiencies have been boosted to as high as 98% [17,18]. In addition, other quantum states (such as entangled coherent states [19], optimal states [20], and other nonclassical states [21,22]) can be used instead, outperforming NOON states while still offering quantum enhancement.

In conclusion, we have realized a proof-of-principle quantum polarized light microscopy that uses $N = 2$ and $N = 3$ NOON states for illumination. We have shown that when limiting detection to only 50 photons per pixel, we were able to improve our phase measurements and thereby the image quality by factors close to $\sqrt{2}$ and $\sqrt{3}$, respectively, as compared with the classical imaging

scheme, bringing this imaging method close to the fundamental Heisenberg limit.

We thank Shlomi Kotler, Lior Cohen, Osip Schwartz, and Oren Raz for fruitful discussions. Financial support of this research by the ERC grant QUAMI, the ICore program of the ISF, the Israeli Nanotechnology FTA program and the Crown Photonics Center is gratefully acknowledged. S. R. and Y. I. contributed equally to this work.

-
- [1] D. J. Stephens and V. J. Allan, *Science* **300**, 82 (2003).
 - [2] K. Eckert, O. Romero-Isart, M. Rodriguez, M. Lewenstein, E. S. Polzik, and A. Sanpera, *Nat. Phys.* **4**, 50 (2007).
 - [3] F. Wolfgramm, C. Vitelli, F. A. Beduini, N. Godbout, and M. W. Mitchell, *Nat. Photonics* **7**, 28 (2012).
 - [4] M. Mitchell, J. Lundeen, and A. Steinberg, *Nature (London)* **429**, 161 (2004).
 - [5] J. Dowling, *Contemp. Phys.* **49**, 125 (2008).
 - [6] I. Afek, O. Ambar, and Y. Silberberg, *Science* **328**, 879 (2010).
 - [7] V. Giovannetti, S. Lloyd, and L. Maccone, *Nat. Photonics* **5**, 222 (2011).
 - [8] G. Brida, M. Genovese, and I. R. Berchera, *Nat. Photonics* **4**, 227 (2010).
 - [9] M. A. Taylor, J. Janousek, V. Daria, J. Knittel, B. Hage, H.-A. Bachor, and W. P. Bowen, *Nat. Photonics* **7**, 229 (2013).
 - [10] T. Ono, R. Okamoto, and S. Takeuchi, *Nat. Commun.* **4**, 3426 (2013).
 - [11] C. K. Hong, Z. Y. Ou, and L. Mandel, *Phys. Rev. Lett.* **59**, 2044 (1987).
 - [12] H. F. Hofmann and T. Ono, *Phys. Rev. A* **76**, 031806 (2007).
 - [13] G. Khoury, H. S. Eisenberg, E. J. S. Fonseca, and D. Bouwmeester, *Phys. Rev. Lett.* **96**, 203601 (2006).
 - [14] R. Okamoto, H. F. Hofmann, T. Nagata, J. L. O'Brien, K. Sasaki, and S. Takeuchi, *New J. Phys.* **10**, 073033 (2008).
 - [15] See Supplemental Material at <http://link.aps.org/supplemental/10.1103/PhysRevLett.112.103604> for a proof of the optimality of the estimators.
 - [16] P. Walther, J.-W. Pan, M. Aspelmeyer, R. Ursin, S. Gasparoni, and A. Zeilinger, *Nature (London)* **429**, 158 (2004).
 - [17] D. Fukuda, G. Fujii, T. Numata, K. Amemiya, A. Yoshizawa, H. Tsuchida, H. Fujino, H. Ishii, T. Itatani, S. Inoue *et al.*, *Opt. Express* **19**, 870 (2011).
 - [18] F. Marsili, V. Verma, J. Stern, S. Harrington, A. Lita, T. Gerrits, I. Vayshenker, B. Baek, M. Shaw, R. Mirin *et al.*, *Nat. Photonics* **7**, 210 (2013).
 - [19] C. C. Gerry and J. Mimih, *Phys. Rev. A* **82**, 013831 (2010).
 - [20] U. Dorner, R. Demkowicz-Dobrzanski, B. J. Smith, J. S. Lundeen, W. Wasilewski, K. Banaszek, and I. A. Walmsley, *Phys. Rev. Lett.* **102**, 040403 (2009).
 - [21] T. Ono and H. F. Hofmann, *Phys. Rev. A* **81**, 033819 (2010).
 - [22] A. Datta, L. Zhang, N. Thomas-Peter, U. Dorner, B. J. Smith, and I. A. Walmsley, *Phys. Rev. A* **83**, 063836 (2011).